Electronic Supplementary Material (ESI) for Chemical Communications.

Electronic Supplementary Information (ESI) for :

Interfacial Engineering of Mo/$Hf_{0.3}Zr_{0.7}O_2$/Si Capacitor Using Direct Scavenging Effect of Thin Ti layer

Se Hyun Kim[a], Geun Taek Yu[a], Geun Hyeong Park[a], Dong Hyun Lee[a], Ju Yong Park[a], Kun Yang[a], Eun Been Lee[a], Je In Lee[a,*] and Min Hyuk Park[a,b,*]

a School of Materials Science and Engineering, Pusan National University, Busan 46241, Republic of Korea.

b Department of Materials Science and Engineering & Inter-University Semiconductor Research Center, College of Engineering, Seoul National University, Seoul, Republic of Korea.

E-mail : jilee@pnu.ac.kr, minhyuk.park@snu.ac.kr

Table of contents :

Experimental section

Before film deposition, native SiO_x was wet-etched using a buffered oxide etchant (BOE) with a 5% hydrofluoric acid solution and an etching time of 30 s. HZO films (10 nm) were deposited using thermal atomic layer deposition (ALD) on highly doped n-type Si (n^+Si, resistivity ρ = 0.005 Ω·cm) at substrate temperatures of 280 °C. $[(CH_3)(C_2H_5)N]_4Hf$ (TEMAH) and $[(CH_3)(C_2H_5)N]_4Zr$ (TEMAZ) were used as the metal precursors, and O_3 was chosen as the oxygen source. The growth of both HfO_2 and ZrO_2 was ~0.096 nm per cycle. The Mo top electrode was deposited via direct current (DC) reactive sputtering with a shadow mask, and a hole diameter of 200 μm was used for patterning. The plasma power, base pressure, and working pressure were 150 W, 3×10^{-6} Torr, and 8×10^{-3} Torr, respectively. The Ti sacrificial layer was deposited via DC reactive sputtering, using three different sputtering times, namely 12, 20, and 25 s. The plasma power, base pressure, and working pressure were 100 W, 3×10^{-6} Torr, and 5×10^{-3} Torr, respectively. For the crystallization of the as-deposited HZO films, rapid thermal annealing (RTA) was conducted at 500 °C for 30 s under a N_2 atmosphere.

Structural properties of the samples with and without Ti sputtering were examined using grazing incidence X-ray diffraction (GIXRD, SmartLab, Rigaku) with a Cu X-ray source using an incidence angle of ω = 0.5°. Schematics of the device structures are shown in Fig. 1a. Transmission electron microscopy (TEM, TALOS F200X, Thermo Fisher Scientific) was used to examine the nanostructures and chemical nature of the samples by adopting energy dispersive spectroscopy (EDS). Electrical measurements were performed using a semiconductor characterization system (4200A-SCS, Keithley) with an SMU module (Keithley), a pulse measurement unit (4225-PMU, Keithley), and an LCR meter (4100, Wayne Kerr Electronics). Bipolar triangular pulses 3.5 V high were used to measure the polarization–voltage (P-V) curve at a measurement frequency of 1 kHz. For the endurance test, 3.5 V-high positive up negative down (PUND) pulses at a 100 kHz frequency were used. Capacitance-voltage (C-V) measurements were carried out using a small-signal voltage amplitude and frequency of 50 mV and 10 kHz, respectively, for DC voltage between -3.5 V and +3.5 V.

Aspect ratio and X-ray diffraction patterns of 12, 20, and 25s Ti samples

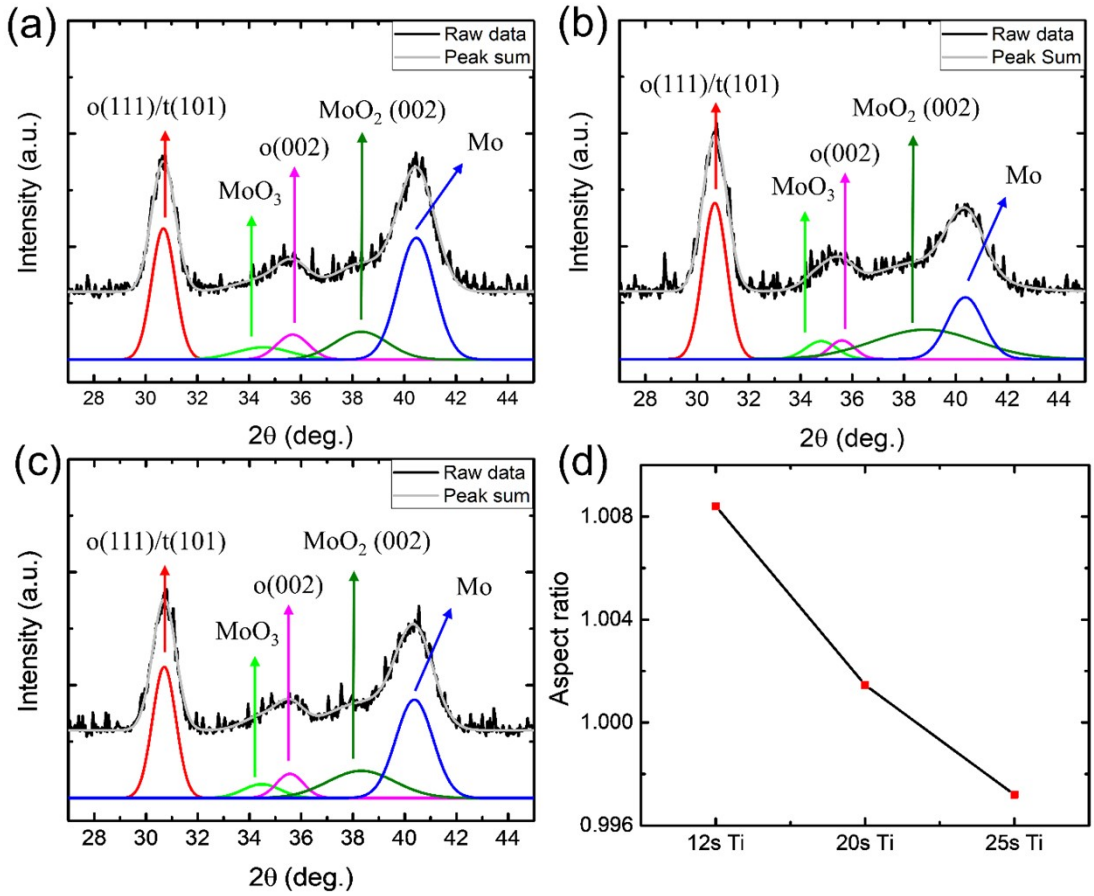

Figure S1. An enlarged grazing incidence X-ray diffraction patterns (GIXRD) from fig. 1(b) with 2θ of 27° to 45°. (a) 12s Ti, (b) 20s Ti and (c) 25s Ti. (d) The aspect ratio (2a/(b+c)) for orthorhombic phase was calculated by Gaussian fitting for the various diffraction peaks from the $Hf_{0.3}Zr_{0.7}O_2$, Mo, MoO_2, and MoO_2.

From fig. S1(a)-(c), o(111)/t(101) 2θ peak positions of 12s, 20s and 25s Ti were 30.68º, 30.68º, 30.70º. And o(002) 2θ peak positions of 12s, 20s and 25s Ti were 35.68º, 35.60º and 35.56º respectively. Lattice parameters a,b, and c were calculated from angles of o(111)/t(101) and o(002) diffraction peaks. And the aspect ratio (2a(b+c)) for the orthorhombic phase were calculated from lattice parameters. In fig. S1. (d), the aspect ratio decreased with increasing Ti sputtering time and the aspect ratio of 25s Ti is the lowest. This aspect ratio change means that changing fractions of orthorhombic phase in $Hf_{0.3}Zr_{0.7}O_2$ films. When the aspect ratio decreases, a fraction of orthorhombic phase in $Hf_{0.3}Zr_{0.7}O_2$ film is also decreased and this is the reason for the lowest P_{sat} values of 25s Ti be shown in fig. 4.

STEM HAADF image and EDS elemental maps

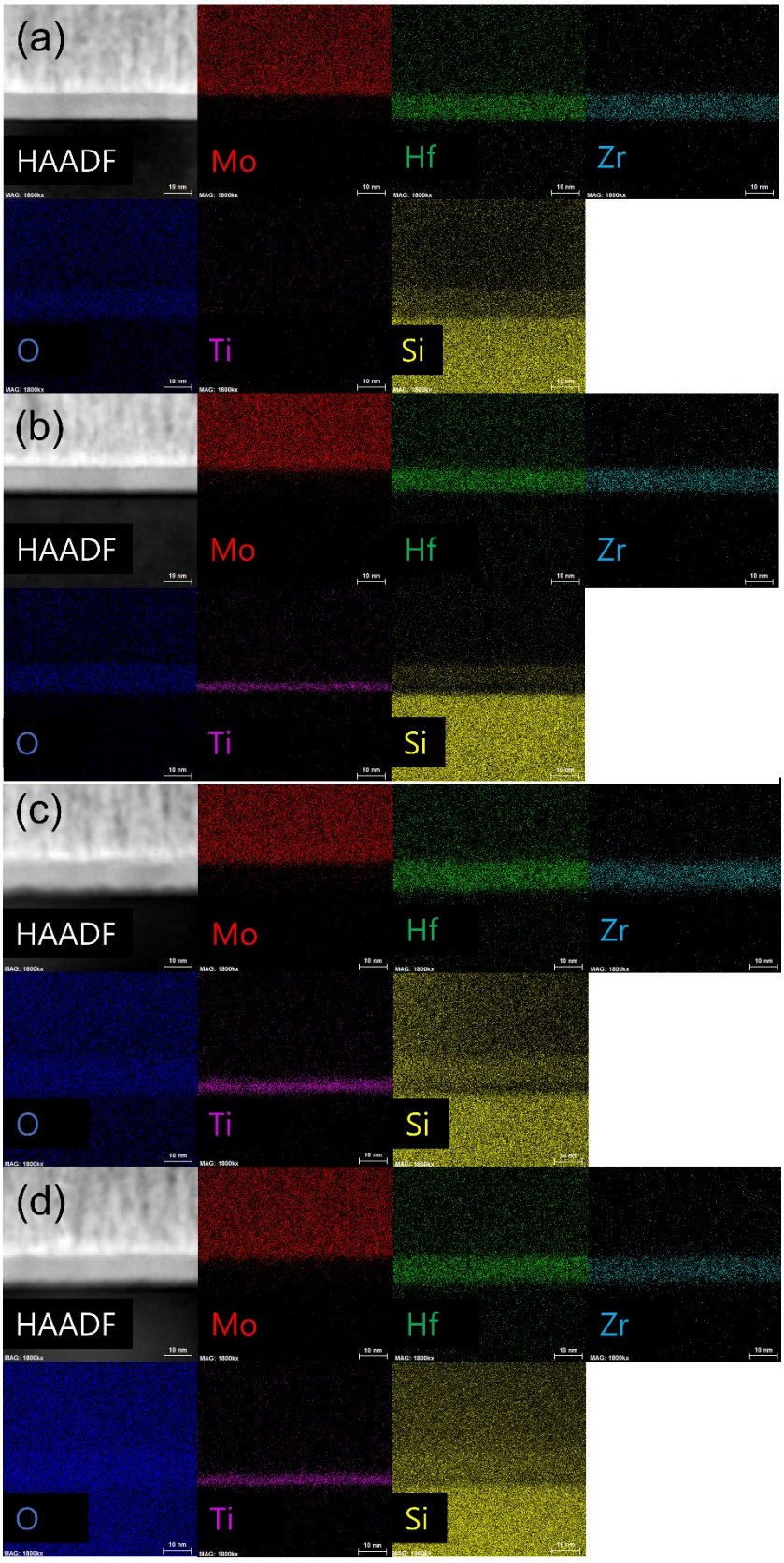

Figure S2. STEM (scanning transmission electron microscopy) HAADF (high angle annular dark field) image and EDS (energy dispersive spectroscopy) elemental maps of (a) Mo/$Hf_{0.3}Zr_{0.7}O_2$/SiO_x/Si capacitor without Ti and (b) Mo/$Hf_{0.3}Zr_{0.7}O_2$/TiO_x/SiO_x/Si capacitor with Ti sputtering time 12 s. (c) Mo/$Hf_{0.3}Zr_{0.7}O_2$/TiO_x/SiO_x/Si capacitor with Ti sputtering time 20 s. (d) Mo/$Hf_{0.3}Zr_{0.7}O_2$/TiO_x/SiO_x/Si capacitor with Ti sputtering time 25 s.

Fig. S2 shows High Angle Annular Dark Field (HAADF) images using the Scanning Transmission Electron Microscopy (STEM) and Electron Dispersive Spectroscopy (EDS) elemental maps of with and without Ti sputtering. Mo appeared in top layer. Below the Mo, Hf and Zr which is solid solution appeared in almost the same region. For different Ti sputtering samples, Ti appeared at the interface between $Hf_{0.3}Zr_{0.7}O_2$ layer and Si substrate. These results indicate that Ti was formed into a thin film despite the short Ti sputtering time.

Electrical properties of Mo/$Hf_{0.3}Zr_{0.7}O_2$/Mo capacitor

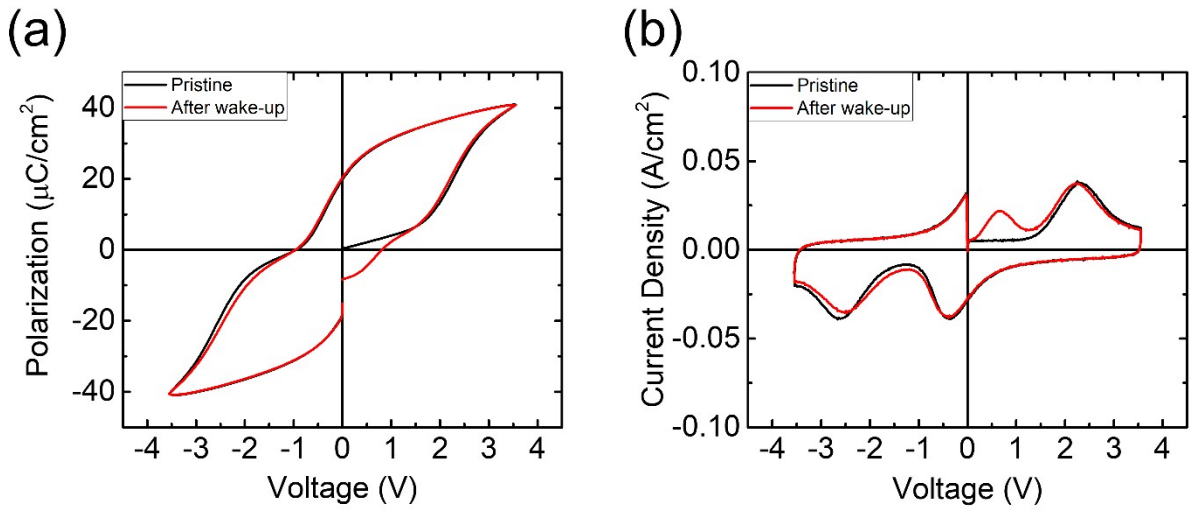

Figure S3. (a) P-V and (b) switching current density-voltage curves of Mo/$Hf_{0.3}Zr_{0.7}O_2$/Mo capacitor. The amplitude of ± 3.5 V with 100 kHz PUND pulses were used to wake-up during 10^3 cycles.

$2V_c$ value of different Zr/(Hf+Zr) ratio of Mo/HZO/SiO_x/n^+Si capacitors

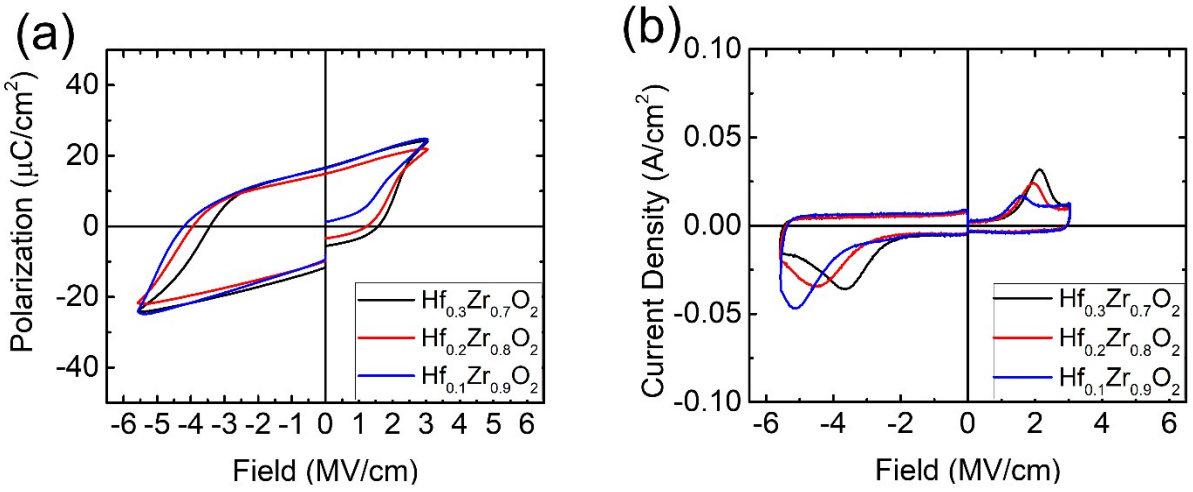

Figure S4. (a) P-V and (b) switching current density-voltage curves of different Zr/(Hf+Zr) ratios of Mo/$Hf_{1-x}Zr_xO_2$/SiO_x/Si capacitors.

Fig. S4a shows ferroelectric-like P-V curve of different Zr/(Hf+Zr) ratios of Mo/HZO/SiO_x/Si capacitors. And From fig. S4b. double coercive voltage ($2V_c$) values of $Hf_{0.3}Zr_{0.7}O_2$, $Hf_{0.2}Zr_{0.8}O_2$, $Hf_{0.1}Zr_{0.9}O_2$ film capacitors are 5.77, 6.44, and 7.75 V, respectively. These two results were evidenced for charge trapping induced by ferroelectric-like behavior. In general study, when Zr/(Hf+Zr) ratio increase 2Vc value was decreased. Opposite about general study Mo/HZO/SiO_x/Si capacitors' 2Vc value increased with increasing Zr/(Hf+Zr) ratio, 0.7 to 0.9.

EDS line scan results

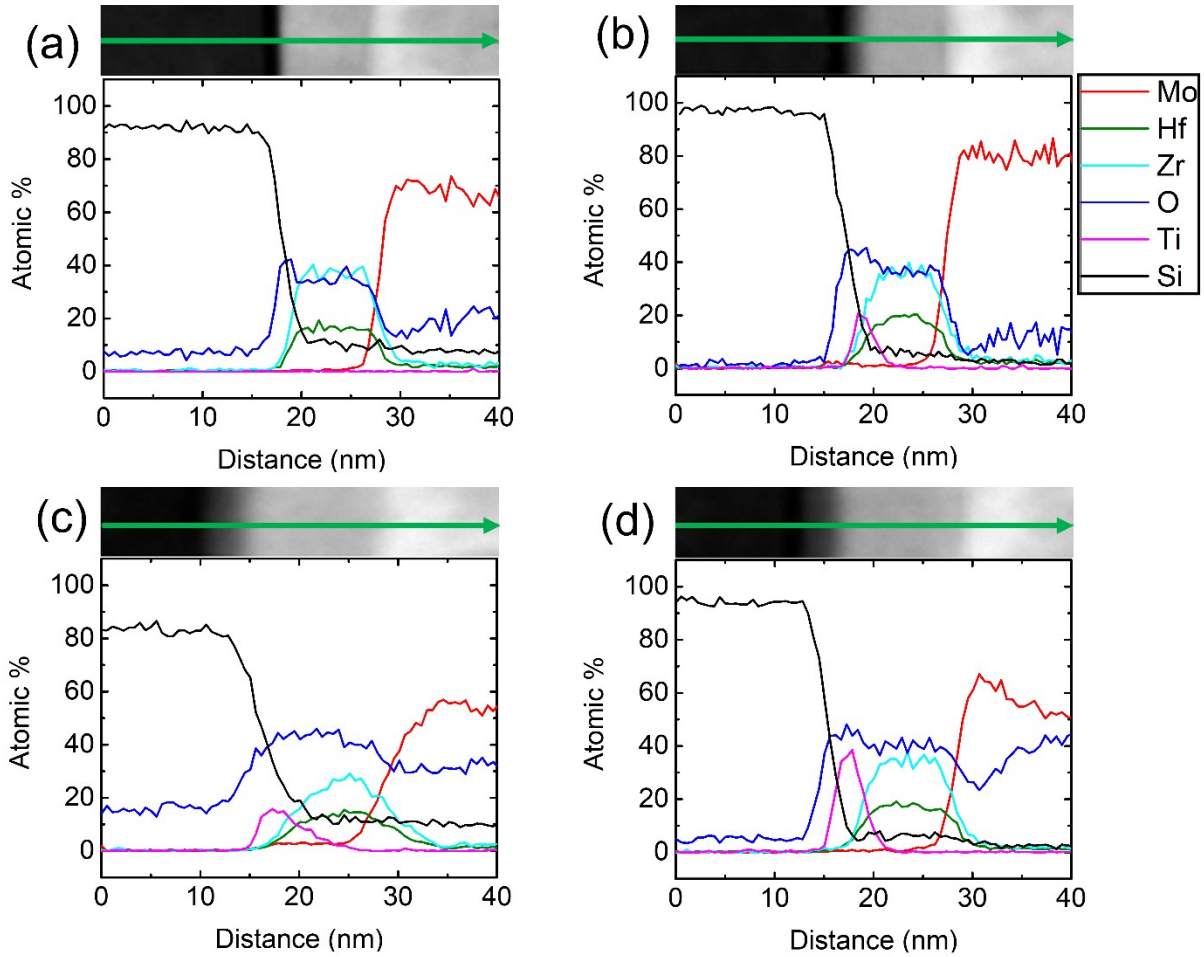

Figure S5. Image of EDS line scan full area and EDS line scan results of (a) No Ti, (b) 12 s Ti, (c) 20 s Ti and (d) 25 s Ti.

In fig. S5a, the atomic % of the elements according to the distance were identified. First, Si appeared and oxidized Hf and Zr appeared in the same region as a solid solution which is comfirmed in fig. S2. In Fig. S5b-d, the other things are the same in fig. S5a, exceptionally, the Ti layer appeared at the HZO/Si interface.

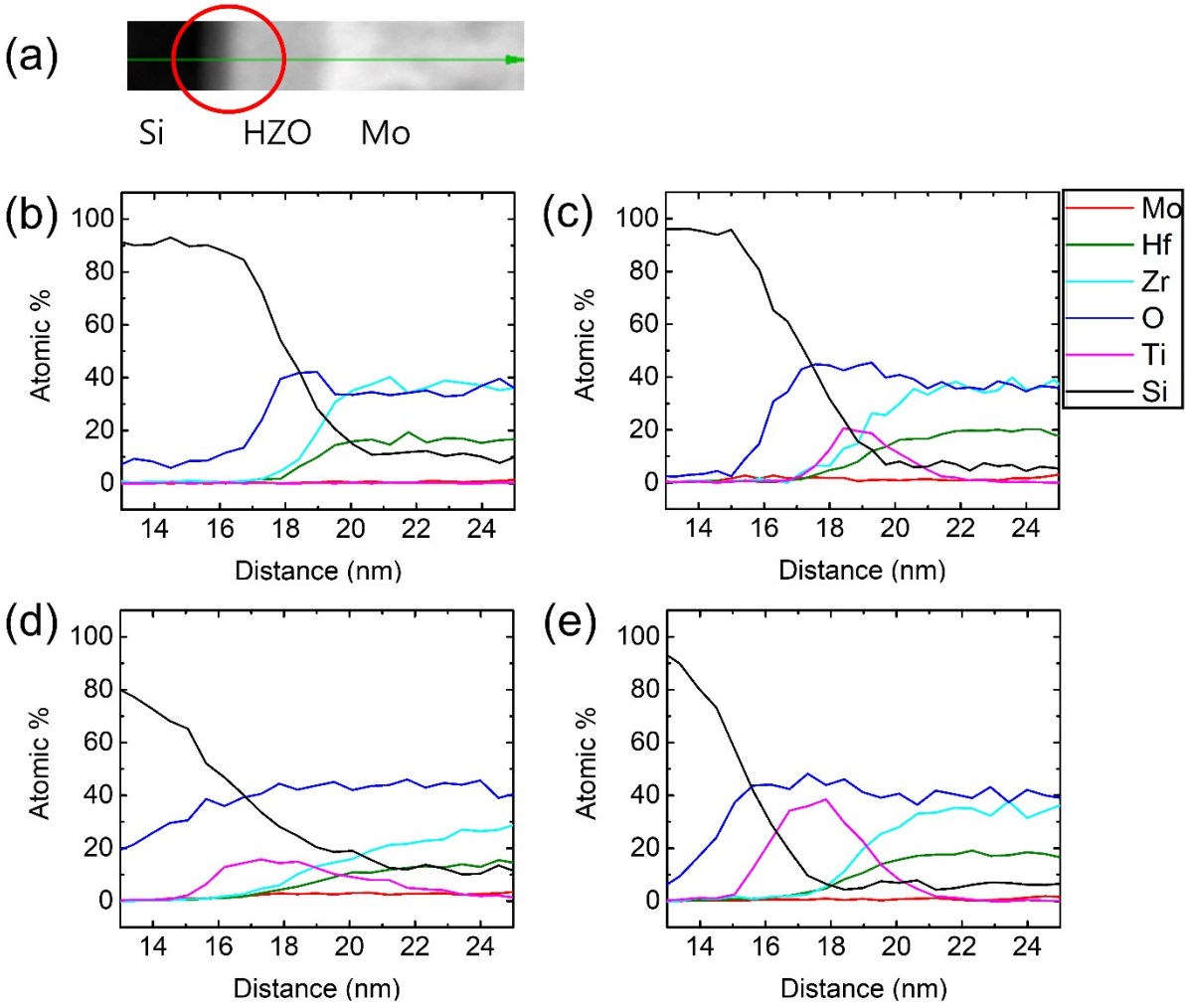

Figure S6. (a) Image of EDS line scan specific area and EDS line scan results of (b) No Ti, (c) 12 s Ti, (d) 20 s Ti and (e) 25 s Ti extrated from fig. S5.

The HZO/Si interface was mainly shown in the results of the entire line scan. In fig. S6b, it can be confirmed that Si was oxidized during the ALD and RTP process so that O and Si exist in the same area. In fig. S6c-e, it can be confirmed that Ti was oxidized and simultaneouly form titanium silicides combined with Si. Therefore (Ti, Si)O_x thin film simultaneously was existed. Ti thickness which is calculated from fig. S6c-d was 2.14, 3.91, and 3.90 nm respectively. The thickness of Ti was overestimated when compared to the results measured from the TEM images.

Endurance test results of $Mo/Hf_{0.3}Zr_{0.7}O_2/SiO_x/Si$ capacitor

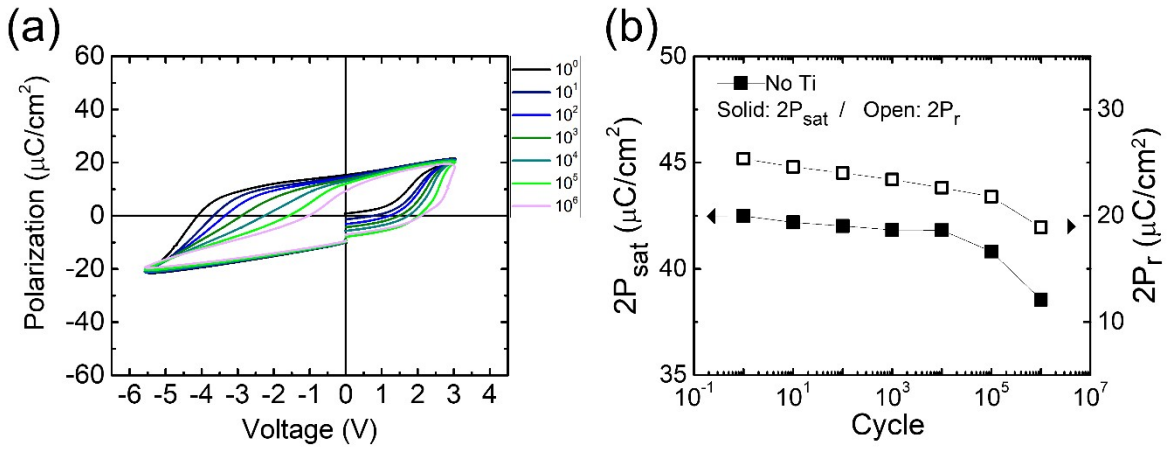

Figure S7. (a) Endurance test results of $Mo/Hf_{0.3}Zr_{0.7}O_2/SiO_x/Si$ capacitor and (b) The doubled saturated polarization ($2P_{sat}$) and doubled remanent polarization ($2P_r$) values extracted from (a) as functions of number of switching cycles.

In fig. S7a as the cycles were applied, the P-V curve of each cycle was collapsed and the $2P_r$ value continued to decrease. In fig. S7b, $2P_r$ and $2P_{sat}$ value were decreased 25.36 to 18.91 $\mu C/cm^2$ (~25 % decreased), 42.49 to 38.56 $\mu C/cm^2$ (~9 % decreased), respectively, after 10^6 cycles. The P-V curve of no Ti did not withstand 10^7 cycles and strong fatigue occurred. It is noticed that the endurance was significantly decreased compared with $Mo/Hf_{0.3}Zr_{0.7}O_2/TiO_x/SiO_x/Si$ capacitors with different Ti sputtering times. These results indicate that Ti sacrificial layer affects operation voltage and increases endurance properties.